Buletin Teknik Elektro dan Informatika
(Bulletin of Electrical Engineering and Informatics)
Vol.1, No.2, June 2012, pp. 89~96
ISSN: 2089-3191

Efficient Closed Form Cut-Off Planes and Propagation Planes Characteristics for Boundary-Value Problems

Junaid Zafar[1], Haroon Zafar[2], Tasneem Zafar[3]
[1]Electromagnetics Research Group, Department of Electrical Engineering, University of Comsats, Lahore, Pakistan, Ph: + 92 (42) 111-001-007
[2] Tissue Optics & Microcirculation Imaging, Department of Electrical & Electronic Engineering, National University of Ireland, Galway, Ireland, Ph: +92 (322) 4641477
[3]Department of Economics, Government College University, Lahore, Pakistan
COMSATS Institute of Information Technology, Defence Road, Off Raiwind Road, Lahore,
Ph: + 92 (42) 35180121, Fax: +92 (42) 9203100
e-mail: junaidzafar@ciitlahore.edu.pk[1]

Abstract

The geometrical relationship between the cut-off and propagating planes of any waveguide system is a prerequisite for any design process. The characterization of cut-off planes and optimisation are challenging for numerical methods, closed-form solutions are always preferred. In this paper, Maxwell's coupled field equations are used to characterise twin E-plane and H-plane slab loaded boundary value problems. The single mode bandwidths and dispersion characteristics of these structures are presented and critically compared. The impact of slab mobility upon cut-off and propagations planes has been envisaged. The presented formulation has been extended further to derive a vectorized Green function expression to link electric and magnetic fields for the characterization of planar waveguide structures.

Keywords*: cut-off plane, propagation plane, mode nomenclature, numerical methods.*

1. Introduction

Dielectric slab loaded waveguide structures are used for wave guiding and frequently exploited in beam accelerating and plasma discharge structures [1-2], impedance matching networks [3], polarizing beam splitters [4] and waveguide filters [5]. Such structures do not support transverse electric (TE) or transverse magnetic (TM) eigen solutions due to interface mismatching. Hybrid modes propagate are labelled as longitudinal sectional electric (LSE) or longitudinal sectional magnetic (LSM) modes. Although numerical techniques, such as the finite element method, are now routinely used to analyse these waveguide structures, closed form methods are always preferred as they are computationally efficient and support both optimization and synthesis. In particular, transcendental equations can be solved for both the cut-off and propagating planes, whereas, numerical methods need to be reformulated and can involve iterative techniques. In this paper, coupled potential field equations in terms of the magnetic and electric vector potentials are used to solve the boundary value problems for E and H-plane loaded waveguides. This routine is computationally efficient and Hertzian potential expressed in terms of sinusoidal functions are used to give a closed form field solution for both LSE and LSM modes. The method is demonstrated for a twin H- plane and E- plane slab loaded rectangular waveguides. By setting the propagation constant to zero, the cut-off plane for these waveguides as a function of geometry are also presented. The planar waveguide structures that include microstrips, coplanar waveguides and slot lines are non- separable structures and each LSE and LSM mode has a scattered distribution pattern exciting a range of other LSE and LSM modes and the composite modal patterns are neither LSE nor LSM. The developed formulation is extended to incorporate both electric and magnetic potentials to devise closed form solution to planar waveguide boundary value problems.

2. Coupled Potential Equations

An electric vector potential (***F***) and a magnetic vector potential (***A***) can be used to define the electric (***E***) and magnetic (***H***) fields in a charge free region. For a mixed representation,

Received February 14, 2012; Revised April 10, 2012; Accepted May 17, 2012

involving both magnetic and electric potentials a pair of coupled equations for E and H follows as:

$$E = \frac{\nabla(\nabla.\vec{A})}{j\omega\mu\varepsilon} - j\omega\vec{A} - \frac{1}{\varepsilon}(\nabla\times\vec{F}) \qquad (1)$$

$$H = \frac{\nabla(\nabla.\vec{F})}{j\omega\varepsilon\mu} - j\omega\vec{F} + \frac{1}{\mu}(\nabla\times\vec{A}) \qquad (2)$$

where ε^* and μ^* are the complex permittivity and permeability respectively.

Table 1. General field solution for H-plane slabs

For H-plane slabs supporting LSM (TM^y) modes the Hertzian magnetic potential is zero and the coupled equations provide:	For the case of LSE (TE^y) modes the Hertzian electric potential is zero and the coupled equations provide:
$E_x = \frac{\partial^2\psi^e}{\partial x\partial y}e^{-j\beta_{mn}z}$	$E_x = \omega\mu_o\beta_{mn}\psi^m e^{-j\beta_{mn}z}$
$E_y = (\frac{\partial^2}{\partial y^2} + \varepsilon_r k_o{}^2)\psi^e e^{-j\beta_{mn}z}$	$E_y = 0$
$E_z = -j\beta_{mn}\frac{\partial\psi^e}{\partial y}e^{-j\beta_{mn}z}$	$E_z = j\omega\mu_o\frac{\partial\psi^m}{\partial x}e^{-j\beta_{mn}z}$
$H_x = -\omega\varepsilon_o\beta_{mn}\psi^e e^{-j\beta_{mn}z}$	$H_x = \frac{\partial^2\psi^m}{\partial x\partial y}e^{-j\beta_{mn}z}$
$H_y = 0$	$H_y = (\frac{\partial^2}{\partial y^2} + \varepsilon_r k_o{}^2)\psi^e e^{-j\beta_{mn}z}$
$H_z = j\omega\varepsilon\frac{\partial\psi^e}{\partial x}e^{-j\beta_{mn}z}$	$H_z = -j\beta_{mn}\frac{\partial\psi^m}{\partial y}e^{-j\beta_{mn}z}$

Table 2. General Field Solution for an E-plane slabs

In the case of E-plane slabs supporting LSE (TE^x) modes, the Hertzian electric potential is zero and coupled equations yield;	For LSM (TM^x) modes we derive;
$E_x = 0$	$E_x = (\frac{\partial^2\psi^e}{\partial x^2} + \varepsilon_r k_o{}^2\psi^e)e^{-j\beta_{mn}z}$
$E_y = \omega\mu_o\beta_{mn}\psi^m e^{-j\beta_{mn}z}$	$E_y = \frac{\partial^2\psi^e}{\partial x\partial y}e^{-j\beta_{mn}z}$
$E_z = -j\omega\mu_o\frac{\partial\psi^m}{\partial y}e^{-j\beta_{mn}z}$	$E_z = -j\beta_{mn}\frac{\partial\psi^e}{\partial x}e^{-j\beta_{mn}z}$
$H_x = (\frac{\partial^2\psi^m}{\partial x^2} + \varepsilon_r k_0{}^2\psi^m)e^{-j\beta_{mn}z}$	$H_x = 0$
$H_y = \frac{\partial^2\psi^m}{\partial x\partial y}e^{-j\beta_{mn}z}$	$H_y = -\omega\varepsilon_o\beta_{mn}\psi^e e^{-j\beta_{mn}z}$
$H_z = -j\beta_{mn}\frac{\partial\psi^m}{\partial x}e^{-j\beta_{mn}z}$	$H_z = j\omega\varepsilon\frac{\partial\psi^e}{\partial y}e^{-j\beta_{mn}z}$

In practice, for dielectric loaded waveguides, $\vec{A}$ is an electric Hertz vector potential ($\vec{A} = j\omega\varepsilon\mu\psi^e$) and $\vec{F}$ is a magnetic Hertz vector potential ($\vec{F} = j\omega\varepsilon\mu\psi^m$). This is a formulation that yields the complete field solution and characteristic equations for slab loaded waveguides. General field solutions for H-plane and E-plane slab loaded structures are illustrated in Table 1 and Table 2.

3. Application to a Twin H-plane Slab Loaded Waveguide

Now consider the twin slab arrangement in Figure 1. For LSE **(**TE^y**)** modes the magnetic potential is defined as;

$$\psi^m(0 \le y \le h) = 1/\ j\omega\mu_o[C_1 \cos(m\pi/a)(x+a/2)\cos k_{y1} y e^{-j\beta_{mn}z}] \quad (3)$$

$$\psi^m(h \le y \le b/2) = 1/\ j\omega\mu_o[D_1 \cos(m\pi/a)(x+a/2)\cos k_{y1} y e^{-j\beta_{mn}z}] \quad (4)$$

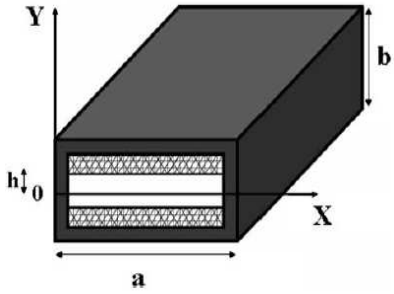

Figure 1. Twin H-Plane slab loaded waveguide.

and by using equation in the first column of Table 1, the electric and magnetic field components follow as;

$$E_x(0 \le y \le h) = -j\beta_{mn} C_1 \cos(m\pi/a)(x+a/2)\cos k_{y1} y e^{-j\beta_{mn}z}$$

$$E_x(h \le y \le b/2) = -j\beta_{mn} D_1 \cos(m\pi/a)(x+a/2)\sin k_{y2}(b/2-y) e^{-j\beta_{mn}z}$$

$$E_y(0 \le y \le h) = 0$$

$$E_y(h \le y \le b/2) = 0$$

$$E_z(0 \le y \le h) = C_1(m\pi/a)\sin(m\pi/a)(x+a/2)\cos k_{y1} y e^{-j\beta_{mn}z}$$

$$E_z(h \le y \le b/2) = D_1(m\pi/a)\sin(m\pi/a)(x+a/2)\sin k_{y2}(b/2-y) e^{-j\beta_{mn}z}$$

$$H_x(0 \le y \le h) = (1/\ j\omega\mu_o)\cdot C_1 k_{y1}(m\pi/a)\sin(m\pi/a)(x+a/2)\sin k_{y1} y e^{-j\beta_{mn}z}$$

$$H_x(h \le y \le b/2) = (1/\ j\omega\mu_o)\cdot D_1 k_{y2}(m\pi/a)\sin(m\pi/a)(x+a/2)\cos k_{y2}(b/2-y) e^{-j\beta_{mn}z}$$

$$H_y(0 \le y \le h) = (1/\ j\omega\mu_o)\cdot C_1 k_c^{\ 2}\cos(m\pi/a)(x+a/2)\cos k_{y1} y e^{-j\beta_{mn}z}$$

$$H_y(h \le y \le b/2) = (1/\ j\omega\mu_o)\cdot D_1 k_c^{\ 2}\cos(m\pi/a)(x+a/2)\sin k_{y2}(b/2-y) e^{-j\beta_{mn}z}$$

$$H_z = (-1/\omega\mu_o)\cdot j\beta_{mn}^{\ 2} C_1 k_{y1}^{\ 2}\cos(m\pi/a)(x+a/2)\sin k_{y1} y e^{-j\beta_{mn}z}$$

$$H_z = (-1/\omega\mu_o)\cdot j\beta_{mn}^{\ 2} D_1 k_{y2}^{\ 2}\cos(m\pi/a)(x+a/2)\cos k_{y2}(b/2-y) e^{-j\beta_{mn}z}$$

and the characteristic equation is derived as:

$$k_{y1}\sin[k_{y2}(b/2-h)]\sin k_{y1}h - k_{y2}\cos(k_{y1}h)\cos[k_{y2}(b/2-h)=0 \quad (5)$$

In the usual way, the transverse propagation constant can be expressed in terms of longitudinal propagation constant as;

$$k_{y1} = \varepsilon_1 k_o^{\,2} - k_c^{\,2} \quad (6)$$

$$k_{y2} = \varepsilon_2 k_o^{\,2} - k_c^{\,2} \quad (7)$$

where $k_o = \frac{\omega}{c}$ is the propagation constant for free space, $k_c^{\,2} = (m\pi/a)^2 + \beta_{mn}^{\,2}$, ε_1 is the air permittivity and ε_2 is the relative dielectric permittivity of the slab loading the waveguide.

Similarly for LSM modes, the potentials are defined as;

$$\psi^e(h \le y \le b/2) = B_1 \sin(m\pi/a)(x+a/2)\cos k_{y2}(b/2-y)e^{-j\beta_{mn}z} \quad (8)$$

$$\psi^e(0 \le y \le h) = A_1 \sin(m\pi/a)(x+a/2)\sin k_{y1} y e^{-j\beta_{mn}z} \quad (9)$$

The field solution can be derived in the usual way and by applying boundary conditions, we determine the dispersion relation as;

$$k_{y2}\sin[k_{y2}(b/2-h)]\sin k_{y1}h - \varepsilon_r k_{y1}\cos(k_{y1}h)\cos[k_{y2}(b/2-h)]=0 \quad (10)$$

4. Application to an E-plane Slab loaded waveguide

Figure 2 illustrates an E-plane slab loaded waveguide and for the LSE *(TE^x)* modes the magnetic potentials are defined as;

$$\psi^m(0 \le x \le t) = 1/\ j\omega\mu_o[A_1 \sin k_{x1} x \cos(n\pi/b)y] \quad (11)$$

$$\psi^m(t \le x \le m) = 1/\ j\omega\mu_o[A_2 \sin k_{x2}(m-x)\cos(n\pi/b)y] \quad (12)$$

$$\psi^m(m \le x \le a) = 1/\ j\omega\mu_o[A_3 \sin k_{x3}(a-x)\cos(n\pi/b)y] \quad (13)$$

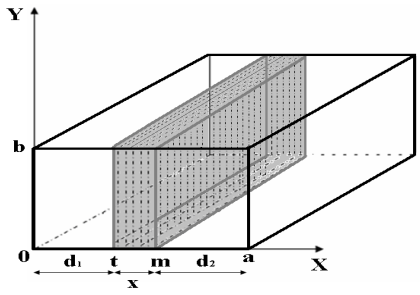

Figure 2. E-Plane slab loaded waveguide.

Using first column expressions in Table 2, the following dispersion relation is obtained after matching boundary conditions across the dielectric interface.

$$\beta_{mn} = \cos k_{x1} a \cos k_{x2} x \sin k_{x1} d_1 / k_{x1} + \sin k_{x2} x / k_{x2} \cdot \cos k_{x1} d_1 + \cos k_{x2} x \cdot \cos k_{x1} d_1 = -\sin k_{x1} d_2 / k_{x1} \cdot$$
$$-k_{x2} \sin k_{x2} x \cdot \sin k_{x1} d_1 / k_{x1} \quad (14)$$

For LSM modes, the final transcendental equation is derived by making use of the second column entries in Table 2.

$$\beta_{mn} = -\cos k_{x1} a \cdot (\cos k_{x2} x \cdot \sin k_{x1} d_1 + k_{x2} / \varepsilon_r \cdot \sin k_{x2} x \cos k_{x1} d_1) + k_{x1} \sin k_{x1} d_2 \cdot (\varepsilon_r k_{x1} / k_{x2} \cdot \sin k_{x2} x$$
$$\sin k_{x1} d_1 - \cos k_{x2} x \cos k_{x1} d_1) = 0 \quad (15)$$

where the transverse propagation constants are given by;

$$k_{x1} = k_{x3} = \varepsilon_1 k_o^{\,2} - \left[\frac{n\pi}{b}\right]^2 - \beta^2_{mn} \quad (16)$$

$$k_{x2} = \varepsilon_2 k_o^{\,2} - \left[\frac{n\pi}{b}\right]^2 - \beta^2_{mn} \quad (17)$$

ε_1 and ε_2 are respected permittivity values for air and the dielectric slab loading the waveguide.

The cut-off plane characteristics for the E-Plane dielectric slab positioned at the waveguide center are presented in Figure 3.

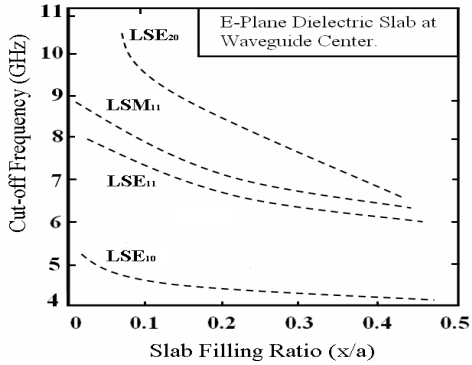

Figure 3 (a). Cut-off frequency against slab filling ratio.
[a = 20.86 mm, b = 10.06 mm, and ε_r = 6].

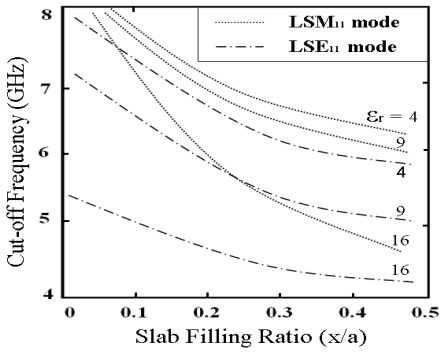

Figure 3 (b). Cut-off frequency against slab filling ratio for LSM_{11} and LSE_{11} modes.

The dominant mode for the configuration presented in Figure 2 is LSE_{10} and the first higher order mode is LSE_{11} that is responsible for limiting the bandwidth. Higher order modes are LSM_{11}, LSE_{20} , LSE_{21} and LSM_{21}. The effect of slab filling ratio upon cut-off frequency for the first two higher order modes is presented in Figure 3 (b). Cut-off frequencies for all modes decrease with the increase in slab filling factor for fixed slab position and dielectric constant. For the fixed values of slab-filling ratios, cut-off frequencies decrease with the increase in dielectric permittivity's and single mode bandwidth increases with it.

Shifting the slab with guide wall results in changing the mode hierarchy to LSE_{10}, LSM_{11}, LSE_{20}, and LSE_{11} as illustrated in Figure 4 (a). The propagation wave number characteristics for air filled region against the slab loaded region are presented in the Figure 4 (b) for different slab positions and filling factors.

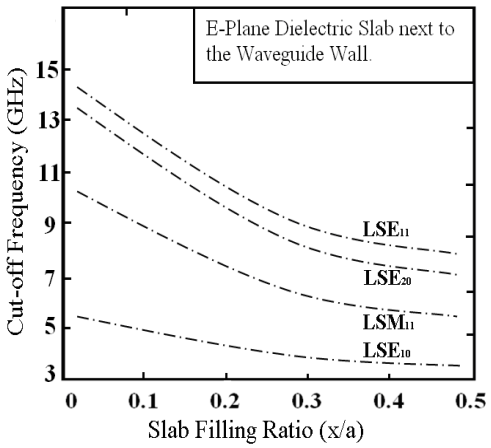

Figure 4 (a). Propagation constant against slab filling ratio.
[a = 20.86 mm, b = 10.06 mm, d_1=0 and x = b and $\varepsilon_{r\,=}$ 4].

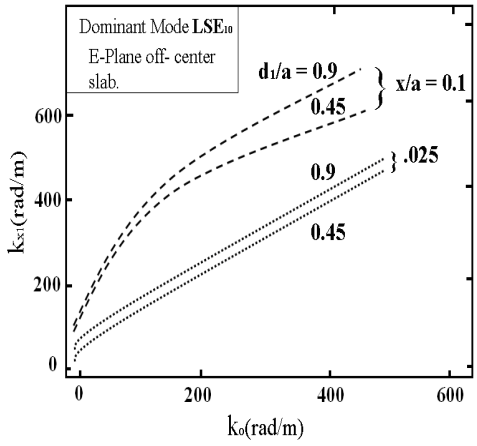

Figure 4 (b). Dielectric region propagation constant against free space propagation constant.

5. Application to Twin Symmetrical E-plane Loaded Waveguide:

Now consider the case of twin symmetrical E-plane slab loaded waveguide structure as illustrated in Figure 5.

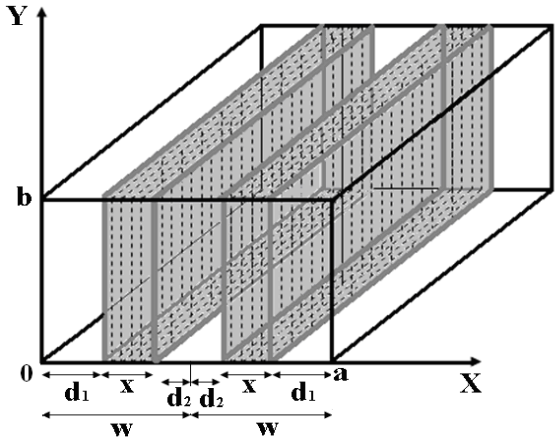

Figure 5. Twin symmetric E- plane slab loaded waveguide.

The cut-off plane characteristics for twin symmetric E-plane slab loaded structure were determined by employing the same formulation and the results are presented in the Figure 6 (a). Figure 6 (a) illustrates the cut-off frequencies depend on the position parameter for different values of dielectric constant and slab filling ratio. The position parameter (d + x/a) gives the distance between the left guide wall and center plane of the left slab as a fraction of half the guide width. The value of this parameter is 0.5 when both slabs are half-way toward each other and (1-x/a) when both slabs are touching each other in the center of guide. When both slabs are touching the guide walls, the position parameter is equal to x/a. A relative comparison is made between the E-plane off-center slab loading to twin symmetrical case for different values of slab filling as presented in Figure 6 (b). The bandwith for twin symmetrical slab loaded structure shows a minimum when the dielectric slab is about 1/4 to 1/3 of the way between waveguide wall and its centre.

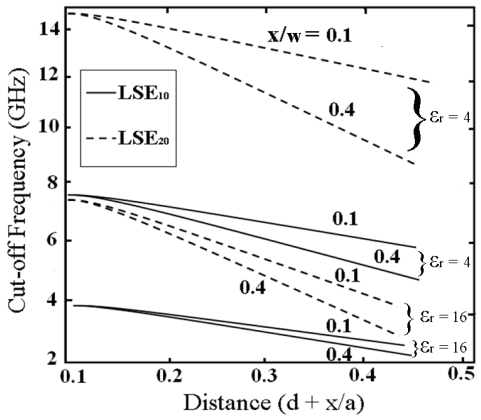

Figure 6 (a). Cut-off frequencies against slab position.

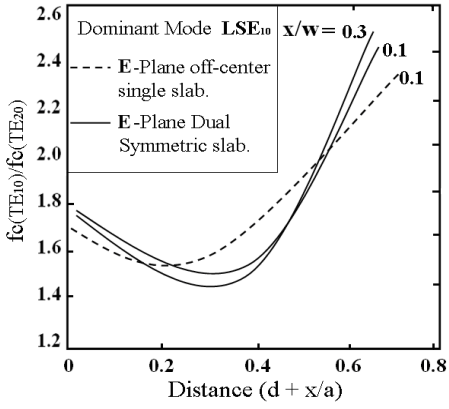

Figure 6 (b). Comparison between off-centre and Twin symmetrical E-plane slab loaded waveguide [$\varepsilon_{r=}$ 9].

6. Derivation of Green Function for Planar Waveguide Structures

In order to derive a Green function to link transverse electric and magnetic field components, the field expressions in column 1 and column 2 of Table 1 are added to form composite field expressions. By expressing the scalar potentials as the superposition of harmonic functions and imposing the appropriate boundary conditions, the transverse electric and magnetic fields expressions as follow;

$$E_x(x,y)=\omega\mu\beta\sum A_n\sqrt{\frac{2}{a}}\cos(\frac{n\pi x}{a})\frac{\sin k_{y1}y}{\sin k_{y1}h}-\sum B_n\frac{n\pi}{a}k_{y1}\sqrt{\frac{2}{a}}\cos(\frac{n\pi x}{a})\frac{\sin k_{y1}y}{\cos k_{y1}h} \quad (18)$$

$$E_z(x,y)=j\omega\mu\sum A_n\frac{n\pi}{a}\sqrt{\frac{2}{a}}\sin(\frac{n\pi x}{a})\frac{\sin k_{y1}y}{\sin k_{y1}h}+j\beta\sum B_n k_{y1}\sqrt{\frac{2}{a}}\sin(\frac{n\pi x}{a})\frac{\sin k_{y1}y}{\cos k_{y1}h} \quad (19)$$

$$H_x(x,y)=\sum -A_n\frac{n\pi}{a}k_{y1}\sqrt{\frac{2}{a}}\sin(\frac{n\pi x}{a})\frac{\cos k_{y1}y}{\sin k_{y1}h}-\omega\varepsilon\beta\sum B_n\sqrt{\frac{2}{a}}\sin(\frac{n\pi x}{a})\frac{\cos k_{y1}y}{\cos k_{y1}h} \quad (20)$$

$$H_z(x,y)=-j\beta\sum A_n k_{y1}\sqrt{\frac{2}{a}}\cos(\frac{n\pi x}{a})\frac{\cos k_{y1}y}{\sin k_{y1}h}+j\omega\varepsilon\sum B_n\frac{n\pi}{a}\sqrt{\frac{2}{a}}\cos(\frac{n\pi x}{a})\frac{\cos k_{y1}y}{\cos k_{y1}h} \quad (21)$$

where A_n and B_n are the projections of the field components on the basis function and can be obtained by computing the inner product of the field components with each function. By expressing these unknown coefficients in terms of transverse electric field components, and by substituting the result in equations (18-21) provides the Green function link transverse field expressions.

$$[H_t(x,y)]=-\int_0^a dx'\begin{pmatrix} -\sum_n \frac{\beta\frac{n\pi}{a}}{\omega\mu k_{y1}}\sqrt{\frac{2}{a}}\sin(\frac{n\pi x}{a})\sqrt{\frac{2}{a}}\cos(\frac{n\pi x'}{a})\cot k_{y1}y & -\sum_n j\frac{\omega^2\mu\varepsilon-(\frac{n\pi}{a})^2}{\omega\mu k_{y1}}\sqrt{\frac{2}{a}}\sin(\frac{n\pi x}{a})\sqrt{\frac{2}{a}}\sin(\frac{n\pi x'}{a})\cot k_{y1}y \\ -\sum_n -j\frac{\omega^2\mu\varepsilon-\beta^2}{\omega\mu k_{y1}}\sqrt{\frac{2}{a}}\cos(\frac{n\pi x}{a})\sqrt{\frac{2}{a}}\cos(\frac{n\pi x'}{a})\cot k_{y1}y & -\sum_n \frac{\beta\frac{n\pi}{a}}{\omega\mu k_{y1}}\sqrt{\frac{2}{a}}\sin(\frac{n\pi x}{a})\sqrt{\frac{2}{a}}\cos(\frac{n\pi x'}{a})\cot k_{y1}y \end{pmatrix}[E_t(x',y)] \quad (22)$$

4. Conclusion

The coupled potential field equations in terms of the magnetic and electric vector potentials are used to solve the boundary value problems for E-plane and H-plane loaded waveguides. The developed formulation has been extended to incorporate both electric and magnetic potentials to characterize planar waveguide boundary value problems.

References

[1] Xiao L, Gai W, Sun X. Field analysis of a dielectric –loaded rectangular waveguide Accelerating structure. *Physical Review E*. 2001: 65; 23-35.

[2] Zafar J, Zafar H, Masood K, Gibson A A P. High emittance electron beam source coupled to slab loaded accelerating structure. *International Journal of Infrared and Millimetre Waves*.2008: 29 (12); 1205-1214.

[3] Zafar J, Gibson A A P, Haigh A, Khairuddin I, Abuelma 'atti A, and Zafar H. E-Plane and H-Plane slab loaded waveguide solutions. *International Journal of Electronics*. 2009: 96 (1); 79-92.

[4] Tyan R C and Salevekar A A. Design, fabrication and characterization of form fringent multilayer polarizing beam splitter. *J. Opt. Soc. Am*. 1997: A-14; 1627-1636.

[5] Mallavarpu R, Asmussen J, and Hawley M C, Behaviour of a microwave cavity discharge over a wide range of pressure and flow rates. *IEEE Trans.Plasma Sci.*1978: 6; 341-354.

[6] Boar G and Zhang W. An Improved Mode matching method for large cavities. *Antennas wireless Propag.Lett*. 2005: 4; 393-396.

[7] Heueh J W and Lin J C. Stable and accurate method for modal analysis of multilayer waveguides using a graph approach. J. Opt. Soc. Am. A. 2007: 24(3); 825-830.

[8] Gardiol F E. Circularly Polarized Electric field in rectangular waveguide. *IEEE Trans. Microwave Theory and Tech.* 1974: 22(5); 563-565.

[9] Tsandoulas G N, Willwerth F G, and Ince W J. LSE_{20} – Mode Characteristics in Phase shifter parametrization. *IEEE Trans. Microwave Theory and Tech.*1972: 20(4); 253-258.

[10] Lee C W, Kim J P. Radiation characteristics of corrugation loaded dielectric-coated conducting cylinder. *IEEE Trans. Antennas Propag*. 2003: 51 (6); 1321–1330.

[11] Matsumoto M, Tsutsumi M, and Kumagai N. Radiation characteristics of a dielectric slab waveguide periodically loaded with thick metal strips. *IEEE Trans. Microwave Theory and Tech*. 1987: 35 (2); 89–95.

[12] Kubo H and Tahara M. Numerical analysis of dielectric- rod waveguides with deep corrugation. *IEEE Trans. Microwave Theory and Tech*. 2002: 50 (5); 1256–1263.